Table 1 Comparison of measured and calculated shock-oscillation frequencies

M_∞	α, deg	M_1	k	f_m, Hz	f_c, Hz
0.688	6.97	1.52	0.507	70	91.3
0.722	6.00	1.47	0.519	75	82.6
0.722	7.02	1.50	0.554	80	75.2
0.732	6.03	1.46	0.513	75	87.8
0.747	4.52	1.42	0.504	75	87.7
0.747	6.04	1.46	0.537	80	85.4
0.747	8.02	1.50	0.505	75	74.1

where M_∞ and M_s are the freestream and airfoil upper surface Mach numbers, respectively. R is a relaxation factor and a value of 0.7 was used based on best correlations with experiments.[7]

Results and Discussion

Knowing a_p and a_u as functions of x, and upon determining x_s and M_c from steady pressure measurements on the airfoil, Eq. (1) can be integrated and the frequency of the feedback loop $f_c = 1/\tau$ is then determined. The results are shown in Table 1 for a few values of M_∞ and α. Considering the uncertainties in locating the shock position x_s and the approximate nature of Eq. (2), the agreement between measured shock frequencies f_m from the balance force spectra and the calculated frequencies f_c is quite good. The maximum Mach number M_1 in front of the shock is also given for reference, since this parameter is sometimes used to indicate the conditions for onset of shock oscillations.[2] The reduced frequencies $k = 2\pi f_m c/U_\infty$ shown in the table are found to be close to the value of 0.4 given by Roos and Riddle[1] for the Whitcomb airfoil.

Conclusions

An analysis of unsteady pressure data from an experimental investigation of a supercritical airfoil showed discrete frequency shock-wave oscillations for certain flow conditions beyond the buffet onset boundary. The time it takes a disturbance to propagate from the shock to the trailing edge plus the additional time it takes for an upstream traveling wave generated at the trailing edge to reach the shock agree quite closely with the period of shock oscillation measured from unsteady force spectra. This supported the proposed mechanism of self-sustained shock motion observed in transonic shock boundary-layer interaction.

References

[1]Roos, F. W. and Riddle, D. R., "Measurements of Surface Pressure and Wake Flow Fluctuations in the Flowfield of a Whitcomb Supercritical Airfoil," NASA TN D-8443, Aug. 1977.

[2]Mabey, D. G., "Oscillatory Flows from Shock-Induced Separations on Biconvex Aerofoils of Varying Thickness in Ventilated Wind Tunnels," AGARD CP-296, Sept. 1980.

[3]McDevitt, J. B., Levy, L. L., Jr., and Deiwert, G. S., "Transonic Flow About a Thick Circular-Arc Airfoil," *AIAA Journal,* Vol. 14, May 1976, pp. 606–613.

[4]Lee, B. H. K. and Ohman, L. H., "Unsteady Pressures and Forces During Transonic Buffeting of a Supercritical Airfoil," *Journal of Aircraft,* Vol. 21, June 1984, pp. 439–441.

[5]Seegmiller, H. L., Marvin, J. G., and Levy, L. L., Jr., "Steady and Unsteady Transonic Flow," AIAA Paper 78-160, Jan. 1978.

[6]Girodroux-Lavigne, P. and Le Balleur, J. C., "Unsteady Viscous-Inviscid Interaction Method and Computation of Buffeting Over Airfoils," Joint IMA/SMAI Conf. on Computational Methods in Aeronautical Fluid Dynamics, Univ. of Reading, MA, April 6–8, 1987.

[7]Tijdeman, H., "Investigations of the Transonic Flow Around Oscillating Airfoils," NLR TR-77090 U, National Aerospace Lab., The Netherlands, 1977.

[8]Ohman, L. H., "The NAE High Reynolds Number 15″ × 60″ Two-Dimensional Test Facility," National Research Council of Canada, NAE-LTR-HA-4, Pt. I, April 1970.

[9]Lee, B. H. K., Ellis, F. A., and Bureau, J., "An Investigation of the Buffet Characteristics of Two Supercritical Airfoils," *Journal of Aircraft,* Vol. 26, Aug. 1989, pp. 731–736.

Vortex Shedding over Delta Wings

O. K. Rediniotis,* H. Stapountzis,†
and
D. P. Telionis‡
Virginia Polytechnic Institute and State University, Blacksburg, Virginia 24061

Introduction

ALL bluff bodies or flat surfaces positioned normal to the oncoming flow alternately shed vortices. These problems have been investigated extensively by researchers interested in flow-induced vibrations, structural mechanics, wind engineering, automobile aerodynamics, and others. Although great interest has been shown today in large-angle-of-attack aerodynamics, the phenomenon of vortex shedding over delta wings has been ignored.

The development of alternate periodic vortex shedding must induce significant asymmetry on the pressure distribution of a wing planform with catastrophic consequences on the stability of an aircraft. However, in most practical cases, this unsteadiness is coupled with the motion of the aircraft, and the interaction is known as wing rock. Alternate shedding of vortices will certainly induce oscillations on a vehicle, but here we are interested in the pure aerodynamic phenomenon of sustained periodic oscillations with a fixed wing. The engineering implications of the present findings are obvious in the case of a dynamic maneuver, which brings a wing at a very large angle of attack, where alternate vortex shedding is unavoidable. The purpose of this research Note is to communicate this preliminary but perhaps significant information.

To confirm the basic concepts, experiments were conducted first with a flat parallelogram and tapered plates positioned normal to the flow. Results on flows over such bodies at large angles of attack are reported in a preliminary report.[1] In the continuation of the work, experiments with delta wings were undertaken. Our findings indicate that for angles of attack up to 35 deg, the leading edge vortices over a delta wing are attached as shown schematically in Fig. 1a. However at higher angles of attack, the leading edge vortices are shed periodically in the wake (see Fig. 1b). Other researchers[2-3] have examined delta wings at angles of attack as high as 80 deg, but so far they have studied only averaged characteristics and apparently have overlooked this dynamic phenomenon. The only contribution that indicated a true search for naturally evolving periodic phenomena is due to Ayoub and McLachlan.[4] These authors observed some periodicity in vortex breakdown but apparently missed the phenomenon of vortex shedding.

Experiments were conducted in the Virginia Polytechnic Institute (VPI) Stability Tunnel and the Engineering Science and Mechanics (ESM) wind tunnel. Measurements were obtained with hot-wire anemometry. The VPI Stability Tunnel is a closed-circuit wind tunnel with a 6×6 ft test section, a very low turbulence level (0.045%), and a maximum attainable speed of almost 200 mph. A mechanism downstream of the model can traverse the hot-wire probes in all three directions. The angle of attack of the wing could be varied between 30

Received April 14, 1989, revision received Sept. 25, 1989.

*Graduate Research Assistant, Department of Engineering Science and Mechanics. Student Member AIAA.

†Assistant Professor, Department of Engineering Science and Mechanics; on leave from the University of Thessaloniki, Greece.

‡Professor, Department of Engineering Science and Mechanics. Associate Fellow AIAA.

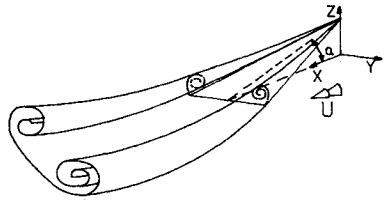

Fig. 1a Schematic of vortex sheets rolling over a delta wing at a moderate angle of attack.

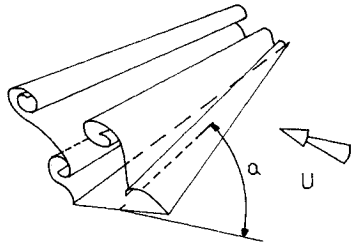

Fig. 1b Schematic of vortical structures shedding alternately over a delta wing at a large angle of attack.

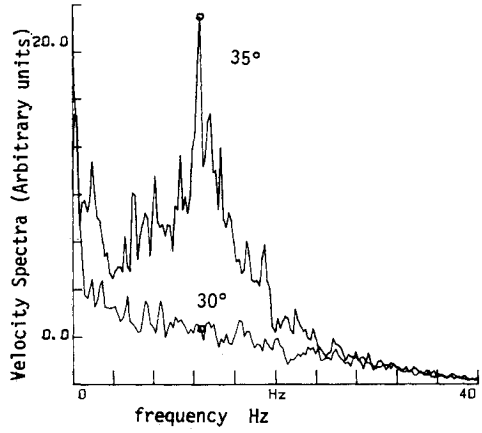

Fig. 2 Velocity spectra in the wake of a delta wing for two different angles of attack (30 and 35 deg) and the same freestream velocity (11.64 m/s); the signal was obtained from a hot-wire probe positioned at $(x, y, z) = (1.7, 0.7, 0.3)$ in the wake of the wing.

and 80 deg and could be adjusted from the control room. The signals were processed by a two-channel signal analyzer (HP 5420A), which displays the response in both time and frequency domain. The ESM wind tunnel is an open-circuit tunnel with a 20×20 in. test section and is provided with a traversing system where the two hot-wire probes were mounted.

Two geometrically similar models were employed with a sweep angle of 76 deg and chord lengths of 304 and 680 mm, respectively. These two models were tested in the ESM tunnel and the VPI tunnel, respectively, to cover a wider range of Reynolds numbers. Coordinates are defined as shown in Fig. 1a. The coordinates of the two hot wires are denoted here by (x_1, y_1, z_1) and (x_2, y_2, z_2), respectively. These lengths are nondimensionalized by the chord length. The two hot wires were positioned symmetrically about the plane of symmetry of the wing, i.e., $y_2 = -y_1$. Their x, y, and z coordinates varied (absolutely) between 1.5 and 2, 0.2 and 0.7, and 0.2 and 0.8, respectively, depending on the angle of attack.

First, the small model was tested in the ESM wind tunnel at Reynolds numbers of order 10^4 to 10^5. These tests indicated some very interesting behavior. For angles of attack less than 37 deg, the velocity spectra in the wake are totally void of any spikes indicating the absence of any organized shedding activity. As the angle of attack increases by about 1 deg, periodic shedding suddenly appears and dominates the wake for all larger angles of attack. The phenomenon proved to be perfectly repeatable: slight changes of the angle of attack below or above the threshold value eliminate or bring back the shedding spike with no hysteresis.

Tests were then repeated in the VPI tunnel with the large model at higher Reynolds numbers, approximately 10^6. The results appear to be nearly independent of the Reynolds number. Again vortex shedding sets in for angles of attack around 35 deg. However, the sharp change of the character of the flow around the value of $\alpha = 37$ deg could not be reproduced. It is possible that in this range of Reynolds numbers, secondary separation is affecting the onset of vortex shedding. Figure 2 shows the velocity spectra in the wake of the wing for two angles of attack around the onset of vortex shedding. In this set of tests, vortex shedding appeared gradually within an increase of the angle of attack of about 3 deg and was firmly established at $\alpha = 35$ deg. The data obtained from both series of experiments (angles of incidence, velocities, and vortex shedding frequencies) have not been corrected for wind tunnel blockage.

The shedding process at high angles of attack, $\alpha = 80$ deg, is confirmed by the response of two hot-wire probes placed downstream of the wing. Figure 3 displays a 180-deg phase

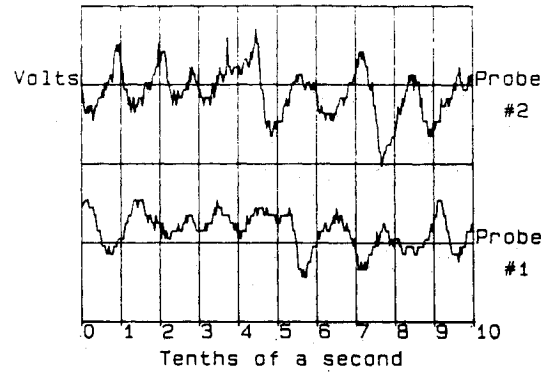

Fig. 3 Time records of the two hot-wire probes positioned at $(x_1, y_1, z_1) = (1.5, 0.3, 0.5)$ and $(x_2, y_2, z_2) = (1.5, -0.3, 0.5)$, respectively, in the wake of the delta wing.

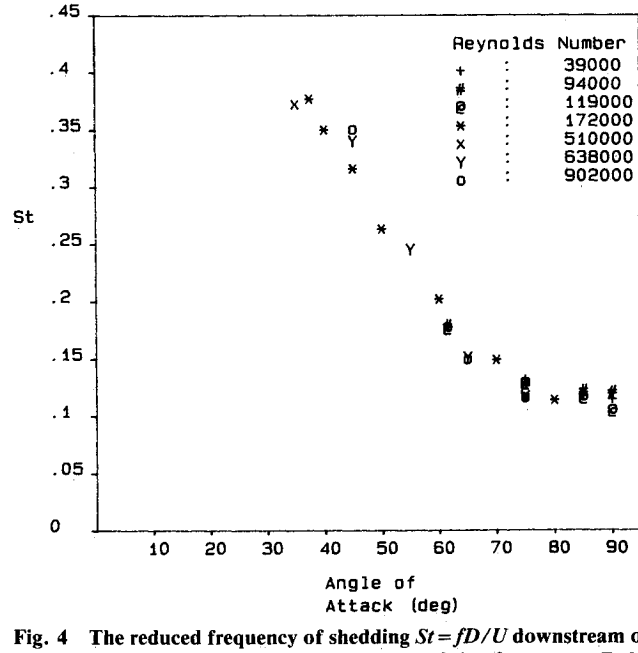

Fig. 4 The reduced frequency of shedding $St = fD/U$ downstream of a delta wing at an angle of attack (f is the shedding frequency, D the wing span, and U the freestream velocity).

difference between the responses of the two probes proving that the vortices are shed alternately.

The reduced frequency of shedding for all the cases vs the angle of attack is plotted in Fig. 4. In this figure we display data obtained from both facilities. There is a very clear dependence of the reduced frequency on the angle of attack. On the other hand, the influence of the Reynolds number is negligible.

The evidence presented here indicates that vortices are shed over delta wings at high angles of attack, just like the cases of other flat surfaces or bluff bodies. Once this aerodynamic phenomenon is set in motion, an aircraft will respond, and interaction between the aerodynamics and the wing attitude will lead to wing rock. However, it should be emphasized that this type of wing rock has not been studied so far. The basic difference with the well-known case is that for very large angles of attack, the flow is fully separated, even if the attitude of the aircraft is fixed.

Since the submission of this research Note, the present team has continued work on this project. Most recently, it was found that at intermediate angles of attack, simultaneous vortex shedding is also possible. The reader will find more information in a recent conference paper.[5]

References

[1]Rediniotis, O., Stapountzis, H., and Telionis, D. P., "Vortex Shedding over Bodies with Non-parallel Edges," Virginia Polytechnic Inst. and State Univ., Blacksburg, VA, Rept. VPI-E-88-89, Dec. 1988.

[2]Malcom, G. N., and Schiff, L. B., "Recent Developments in Rotary-Balance Testing of Fighter Aircraft Configurations at NASA Ames Research Center,"

[3]Brandon, J. M., and Shah, G. H., "Effect of Large Amplitude Pitching Motion on the Unsteady Aerodynamic Characteristics of Flat-plate Wings," AIAA Paper 88-4331-CP, 1988.

[4]LeMay, S. P., Batill, S. M., and Nelson, R. C., "Leading Edge Vortex Dynamics on a Pitching Delta Wing," AIAA Paper 88-2559-CP, 1988.

[5]Ayoub, A., and McLachlan, B. G., "Slender Delta Wing at High Angles of Attack—a Flow Visualization Study," AIAA Paper 87-1230, 1987.

[6]Rediniotis, O. K., Telionis, D. P., and Stapountzis, H., "Periodic Vortex Shedding Over Delta Wings," AIAA Paper 89-1923, 1989.

Postbuckling Analysis of Trusses with Various Lagrangian Formulations

Yeong-Bin Yang* and Liang-Jenq Leu†
National Taiwan University,
Taipei, Taiwan, Republic of China

Introduction

THIS Note is concerned with the incremental nonlinear analysis of elastic trusses involving large strains. First, it will be pointed out that use of the same material constants in an incremental anlaysis does not imply identical material behaviors for the total (TL), updated (UL), and general (GL) Lagrangian formulations. Second, in calculating the bar forces with an incremental analysis, the "total form," rather than the "incremental form," should be used, so as to avoid possible errors.

Received May 11, 1989; revision received June 30, 1989.

*Professor, Department of Civil Engineering
†Graduate Research Assistant, Department of Civil Enginering.

In an incremental formulation, three configurations are needed to describe the motion of a body, i.e., the initial undeformed configuration C_0, current (known) deformed configuration C_1, and a neighboring (desired) deformed configuration C_2. In the TL formulation, C_0 is chosen as the reference, whereas in the UL formulation C_1 is used. Both the TL and UL formulations can be considered as special cases of a GL formulation that adopts an arbitrary known configuration C_m between C_0 and C_1 as the reference.[1] General discussions of the Lagrangian procedures can be found in Refs. 2 and 3. In this Note, left superscripts and subscripts will be used to indicate the occurring and measuring configurations of a quantity, respectively. An incremental quantity between C_1 and C_2 will be denoted with no left superscripts. The following symbols are used in the present discussions: A = sectional area of bar; L = bar length; S = second Piola-Kirchhoff stress; x = axial coordinate, ϵ = Green-Lagrange strain; ρ = specific mass of materials; and τ = Cauchy stress.

Incremental Constitutive Laws

Conventionally, the material law has been expressed in the following incremental form:

$$\text{TL}:{}_0S = F'\left({}^1_0\epsilon\right)_{0}\epsilon \tag{1a}$$

$$\text{UL}:{}_1S = f'\left({}^1_0\epsilon\right)_{1}\epsilon \tag{1b}$$

$$\text{GL}:{}_mS = f'\left({}^1_0\epsilon\right)_{m}\epsilon \tag{1c}$$

where f is a single-valued function and $(')$ is the derivative with respect to the strain ${}^1_0\epsilon$. It is possible to integrate the preceding incremental laws to obtain expressions in terms of the total stresses and strains. By so doing, one may see that the material behaviors implied by Eqs. (1) are very different for large strain problems, as will be demonstrated later.

Formulations with Infinitesimal Step Sizes

Consider a bar that is stretched with an infinitely large number of infinitesimal steps from C_0 to C_2. Let C_i denote an arbitrary configuration of the bar between C_0 and C_2.

TL Formulation

In this case, the strain and stress increments, ${}_0\epsilon$ and ${}_0S$, should be interpreted as the increments from C_i to an infinitesimally close neighboring state. The total stress can be obtained by integration:

$${}^2_0S = \int {}_0S = \int_0^{{}^2_0\epsilon} f'\left({}^1_0\epsilon\right)_{0}\epsilon \tag{2}$$

Noting that ${}^2\rho/{}^0\rho = {}^0A\,{}^0L/({}^2A\,{}^2L)$ for conserved mass and $\partial^2 x/\partial^0 x = {}^2L/{}^0L$, one can relate the Cauchy stress ${}^2\tau$ to the second Piola-Kirchhoff stress ${}^2_0S$ as follows[2,3]:

$$2\tau = {}^2_0S\,{}^0A\,{}^0L/({}^2A\,{}^0L) \tag{3}$$

Consequently, the axial force ${}^2_2F$ at C_2 can be obtained:

$${}^2_2F = 2_\tau\,{}^2A = {}^2_0S\,{}^0A\,({}^2L/{}^0L) \tag{4}$$

UL Formulation

For the purpose of obtaining closed-form expressions, one may convert the UL formulations, with moving coordinates, into an equivalent TL formulation, with a fixed reference. The stress increment for the UL formulation is ${}_iS = E_i\epsilon$, which is